ACS OMEGA

http://pubs.acs.org/journal/acsodf

Article

Synthesis and Characterization of $^{15}N_5$-Labeled Aflatoxin B_1−Formamidopyrimidines and Aflatoxin B_1−N7-Guanine from a Partial Double-Stranded Oligodeoxynucleotide as Internal Standards for Mass Spectrometric Measurements

Pawel Jaruga,* Rachana Tomar, Melis Kant, Vladimir Vartanian, Benjamin Sexton, Carmelo J. Rizzo, Robert J. Turesky, Michael P. Stone, R. Stephen Lloyd, and Miral Dizdaroglu*

Cite This: *ACS Omega* 2023, 8, 14841−14854

Read Online

ACCESS | Metrics & More | Article Recommendations

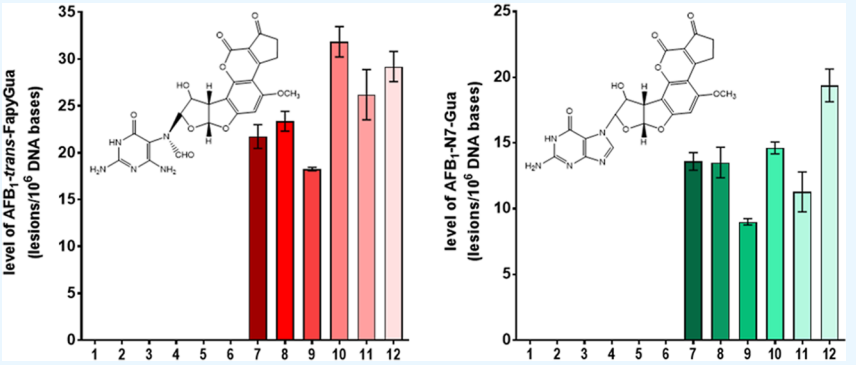

ABSTRACT: Aflatoxin B_1 (AFB_1) exposure through contaminated food is a primary contributor to hepatocellular carcinogenesis worldwide. Hepatitis B viral infections in livers dramatically increase the carcinogenic potency of AFB_1 exposures. Liver cytochrome P450 oxidizes AFB_1 to the epoxide, which in turn reacts with N7-guanine in DNA, producing the cationic *trans*-8,9-dihydro-8-(N7-guanyl)−9-hydroxyaflatoxin B_1 adduct (AFB_1−N7-Gua). The opening of the imidazole ring of AFB_1−N7-Gua under physiological conditions causes the formation of the *cis*- and *trans*-diastereomers of 8,9-dihydro-8-(2,6-diamino-4-oxo-3,4-dihydropyrimid-5-yl-formamido)−9-hydroxyaflatoxin B_1 (AFB_1−FapyGua). These adducts primarily lead to G → T mutations, with AFB_1−FapyGua being significantly more mutagenic than AFB_1−N7-Gua. The unequivocal identification and accurate quantification of these AFB_1−Gua adducts as biomarkers are essential for a fundamental understanding and prevention of AFB_1-induced hepatocellular carcinogenesis. Among a variety of analytical techniques used for this purpose, liquid chromatography−tandem mass spectrometry, with the use of the stable isotope-labeled analogues of AFB_1−FapyGua and AFB_1−N7-Gua as internal standards, provides the greatest accuracy and sensitivity. *cis*-AFB_1−FapyGua-$^{15}N_5$, *trans*-AFB_1−FapyGua-$^{15}N_5$, and AFB_1−N7-Gua-$^{15}N_5$ have been synthesized and used successfully as internal standards. However, the availability of these standards from either academic institutions or commercial sources ceased to exist. Thus, quantitative genomic data regarding AFB_1-induced DNA damage in animal models and humans remain challenging to obtain. Previously, AFB_1−N7-Gua-$^{15}N_5$ was prepared by reacting AFB_1-*exo*-8,9-epoxide with the uniformly $^{15}N_5$-labeled DNA isolated from algae grown in a pure ^{15}N-environment, followed by alkali treatment, resulting in the conversion of AFB_1−N7-Gua-$^{15}N_5$ to AFB_1−FapyGua-$^{15}N_5$. In the present work, we used a different and simpler approach to synthesize *cis*-AFB_1−FapyGua-$^{15}N_5$, *trans*-AFB_1−FapyGua-$^{15}N_5$, and AFB_1−N7-Gua-$^{15}N_5$ from a partial double-stranded 11-mer Gua-$^{15}N_5$-labeled oligodeoxynucleotide, followed by isolation and purification. We also show the validation of these $^{15}N_5$-labeled standards for the measurement of *cis*-AFB_1−FapyGua, *trans*-AFB_1−FapyGua, and AFB_1−N7-Gua in DNA of livers of AFB_1-treated mice.

INTRODUCTION

Aflatoxin toxicity is a worldwide problem leading to hepatocellular carcinomas (HCCs), with more than 850,000 deaths each year, mainly in developing countries of Asia and sub-Saharan Africa, with rising incidences in the USA and Central

Received: February 27, 2023
Accepted: March 20, 2023
Published: April 11, 2023

and South America as well (reviewed in refs 1−6). In 1993, the International Agency for Research on Cancer (IARC) (https://www.iarc.who.int) classified aflatoxin as a "known human carcinogen." Aflatoxins comprise a group of closely related molecules that are readily distinguishable based on their spectral properties and are classified as aflatoxin B_1 (AFB_1), aflatoxin B_2 (AFB_2), aflatoxin G_1 (AFG_1), and aflatoxin G_2 (AFG_2), produced by the fungal strains *Aspergillus parasiticus* and *Aspergillus flavus*. Human exposure to these fungi arises from the consumption of fungal-contaminated staple grains, corn, rice, nuts, cereal crops, and other agricultural products. When compared to other aflatoxins, AFB_1 is the most potent hepatocarcinogen.[2,3,6−11] The carcinogenic potency of AFB_1 is dramatically increased in livers with hepatitis B viral infections.[12−14] Although the liver is the main target of AFB_1, other organs such as kidneys, colon, and lungs may also be affected.[5,15−17] In the liver, AFB_1 undergoes a two-electron oxidation at the 8,9-position generating *exo*- and *endo*-epoxides by cytochrome P450 (CYP) bioactivation, predominantly by CYP3A4 and CYP1A2.[18] The 8,9-*exo*-epoxide reacts with the N7 of guanine in DNA to produce the cationic *trans*-8,9-dihydro-8-(N7-guanyl)−9-hydroxyaflatoxin B_1 adduct (AFB_1−N7-Gua).[19−21] Under physiological conditions, AFB_1−N7-Gua in DNA reacts with water and undergoes opening of the imidazole ring, leading to the formation of the chemically more stable 8,9-dihydro-8-(2,6-diamino-4-oxo-3,4-dihydropyrimid-5-yl-formamido)−9-hydroxyaflatoxin B_1 (AFB_1−FapyGua).[22−24] Depurination of AFB_1−N7-Gua also takes place as a competing pathway.[23,25] In DNA, AFB_1−FapyGua exists as the α- and β-anomers of its 2′-deoxynucleoside, α-AFB_1−FapydG and β-AFB_1−FapydG, with the α-anomer favored in the single-stranded DNA and the β-anomer dominating in the double-stranded DNA.[24] When released from DNA under acidic conditions, AFB_1−FapyGua was shown by nuclear magnetic resonance spectroscopy to exist in four stereoisomeric forms; however, only two forms can be separated by high-performance liquid chromatography (HPLC).[26,27] In subsequent studies, the separable forms were shown to be R_a (*trans*) and S_a (*cis*) C5−N^5-atropisomers, with the former being more dominant than the latter and the formyl group preferentially adopting the *Z* geometry in both atropisomers.[24]

AFB_1 adducts are highly mutagenic, with the mutational signatures dominated by G → T transversion mutations.[4−6,28−33] Both AFB_1−N7-Gua and AFB_1−FapyGua pair with non-cognate adenine and primarily lead to G → T mutations. Low levels of G → A transition mutations (<10%) also occur. However, in both prokaryotic and eukaryotic assays, AFB_1−FapyGua is significantly more mutagenic than AFB_1−N7-Gua. Among the anomeric 2′-deoxynucleoside forms of AFB_1−FapyGua, β-AFB_1−FapydG is a major contributor to mutagenesis, whereas α-AFB_1−FapydG is a strong block to replication.[6,24,29,30,33−35] Based on available data, AFB_1−FapyGua is likely to be the major contributor to genotoxicity of AFB_1 and, by inference, carcinogenesis.

As with other bulky adducts, AFB_1−N7-Gua and AFB_1−FapyGua are substrates for the nucleotide-excision repair (NER) pathway in *Escherichia coli* and mammalian cells.[36,37] Although several investigations have explored a role for base excision repair of aflatoxin adducts in *E. coli*, the data have been inconclusive.[4,37,38] In contrast, studies using human endonuclease VIII-like 1 (NEIL1) revealed that in addition to the well-known incision of the hydroxyl radical-induced 2,6-diamino-4-hydroxy-5-formamidopyrimidine (FapyGua) and 4,6-diamino-5-formamidopyrimidine (FapyAde),[39,40] both unedited NEIL1 (K242) and edited NEIL1 (K242R) recognize and excise AFB_1−FapyGua from multiple sequence contexts in oligodeoxynucleotides and genomic DNAs.[4,41−44] Moreover, *Neil1*$^{-/-}$ mice treated with AFB_1 accumulated significantly greater levels of AFB_1−FapyGua in their liver DNA and developed HCCs at frequencies higher than wild-type or NER-deficient *Xpa*$^{-/-}$ mice.[41] Among human populations, there are known polymorphic variants of NEIL1 with altered DNA glycosylase, β-elimination, and δ-elimination activities.[45−47] Data suggest that individuals carrying the variants of NEIL1 with reduced or no catalytic activity may be at an elevated risk of AFB_1-induced HCCs.

Reliable methods that unequivocally identify and accurately quantify AFB_1−N7-Gua and *cis*- and *trans*-diastereomers of AFB_1−FapyGua as exposure biomarkers will advance basic and applied research into aflatoxin-induced carcinogenesis and in prevention, clinical, and intervention trials (reviewed in refs 5 and 6). The AFB_1−Gua adducts have been measured using a variety of analytical techniques; however, these early studies lacked sufficient positive identification and accurate quantification and could not measure the individual diastereomers of AFB_1−FapyGua[19,21,48−54] (reviewed in ref 5). Later, liquid chromatography−tandem mass spectrometry (LC−MS/MS) was applied to measure AFB_1−N7-Gua and AFB_1−FapyGua in rat urine using aflatoxin B_2 as an internal standard.[55] Subsequently, an improved LC−MS/MS method was reported that used $^{15}N_5$-labeled AFB_1−N7-Gua (AFB_1−N7-Gua-$^{15}N_5$) as an internal standard to measure AFB_1−N7-Gua in human urine.[56] A recent study significantly improved the measurement of the AFB_1−Gua adducts with the simultaneous identification and quantification of *cis*-AFB_1−FapyGua, *trans*-AFB_1−FapyGua, and AFB_1−N7-Gua in DNA of mouse livers using LC−MS/MS and *cis*-AFB_1−FapyGua-$^{15}N_5$, *trans*-AFB_1−FapyGua-$^{15}N_5$, and AFB_1−N7-Gua-$^{15}N_5$ as internal standards.[57]

The use of stable isotope-labeled analogues of the AFB_1−Gua adducts as internal standards is essential for the positive identification and accurate quantification of the individual isomers of the AFB_1−Gua adducts by MS techniques in biological samples such as DNA and urine. Quantitative genomic data regarding AFB_1-induced DNA damage in animal models and humans remain challenging to obtain, in part, because of the limited availability of isotopically labeled standards for the quantification of MS data. The stable isotope-labeled standards, that is, *cis*-AFB_1−FapyGua-$^{15}N_5$, *trans*-AFB_1−FapyGua-$^{15}N_5$, and AFB_1−N7-Gua-$^{15}N_5$, from previous studies are no longer available in any academic research laboratory or commercially. In this work, we report on the synthesis, isolation, purification, and characterization of these stable isotope-labeled standards. We also confirm the usefulness of these standards for measuring *cis*-AFB_1−FapyGua, *trans*-AFB_1−FapyGua, and AFB_1−N7-Gua adducts in vivo in liver DNA of AFB_1-treated mice.

MATERIALS AND METHODS

Ethics Statement. The breeding and care of *Neil1* knockout mice was performed using pre-approved protocols through the Oregon Health & Science University Institutional Animal Care and Use Committee and monitored by the Department of Comparative Medicine.

Materials. An unmodified oligodeoxynucleotide, 5′-d(CCATCGCTACC)-3′, was purchased from the Integrated DNA Technologies, Inc. (Coralville, IA). $^{15}N_5$-2′-Deoxyguano-

https://doi.org/10.1021/acsomega.3c01328
ACS Omega 2023, 8, 14841−14854

sine phosphoramidite was purchased from Cambridge Isotope Laboratories, Inc. (Tewksbury, MA). AFB_1 was purchased from Sigma-Aldrich Chemical Co. (St. Louis, MO). Caution: AFB_1 is a potent liver toxin and is a human carcinogen. *Crystalline AFB_1 is particularly hazardous due to its electrostatic nature and, therefore, should be handled using appropriate containment procedures in a well-ventilated hood and by wearing a respiratory mask to prevent inhalation. AFB_1 can be destroyed by oxidation with NaOCl. It should be presumed that AFB_1-exo-8,9-epoxide is also toxic and a human carcinogen; hence, manipulations should be carried out with suitable containment procedures.*

Synthesis of Oligodeoxynucleotides. The oligodeoxynucleotides with the sequence 5′-d(CCATC**G**CTACC)-3′ were synthesized on a PerSeptive Biosystems model 8909 DNA synthesizer on a 1 μmol scale using Expedite reagents (Glen Research, Sterling, VA) with the standard synthetic protocol for the coupling of the unmodified bases. The coupling of the uniformly labeled $^{15}N_5$-2′-deoxyguanosine phosphoramidite with an N^2-isobutyryl protecting group was performed offline for 30 min.[58] The remainder of the synthesis was performed online using standard protocols. The oligodeoxynucleotide 5′-d(CCATC$^{15}N_5$-**G**CTACC)-3′ was cleaved from the solid support and deprotected with concentrated ammonium hydroxide at 60 °C for 3 h. Both unlabeled and ^{15}N-labeled oligodeoxynucleotides were purified by HPLC using 0.1 mol/L ammonium formate (solvent A) and acetonitrile (solvent B) on a new C-18 reversed-phase semi-preparative column (Clarity C18, 250 mm × 10 mm, Phenomenex, Inc., Torrance, CA) with UV detection at a flow rate of 2 mL/min. The solvent gradient was as follows: initially 99% solvent A; then a 15 min linear gradient to 90% solvent A; then a 4.9 min linear gradient to 80% solvent A; then a 1 min linear gradient to 100% solvent B; 7.4 min isocratic at 100% solvent B; then 1 min linear gradient to 99% solvent A (initial conditions); 5 min isocratic at 99% solvent A to re-equilibrate the column.

Preparation of the AFB_1−Gua Adduct-Containing Oligodeoxynucleotides. The overall experimental design for the synthesis of unlabeled, site-specifically modified oligodeoxynucleotides containing aflatoxin adducts has been previously described.[59] This strategy was followed for the production of both ^{15}N-labeled and unlabeled AFB_1−FapyGua- and AFB_1−N7-Gua-containing oligodeoxynucleotides. The 11-mer single-stranded oligodeoxynucleotides were purified by HPLC using 0.1 mol/L ammonium formate (solvent A) and acetonitrile (solvent B) on a separate column but with similar specifications, that is, a C-18 reverse-phase semi-preparative column (Clarity C18, 250 mm × 10 mm, Phenomenex, Inc., Torrance, CA) with UV detection at 2 mL/min flow rate. The solvent gradient was as follows: initially 94% solvent A; then a 25 min linear gradient to 89% solvent A; then 1 min linear gradient to 94% solvent A (initial conditions); 5 min isocratic at 94% solvent A to re-equilibrate the column. As an additional requirement for the preparation of partial duplex AFB_1−Gua adduct-containing oligodeoxynucleotides, a short oligodeoxynucleotide, 5′-d(TAGCGA)-3′, was also purified under similar conditions as the unlabeled 11-mer oligodeoxynucleotide. Using a short complementary scaffold instead of full complementary oligodeoxynucleotides, which relatively contained more guanines, reduced the complexity due to multiple product formation, thus facilitating subsequent purification steps. Dimethyldioxirane (DMDO), which was required for the oxidation of AFB_1, was synthesized as described.[60] Freshly prepared DMDO (in acetone) was stored with heat-activated molecular sieves (0.5 nm) to absorb water at −20 °C.[60] AFB_1 was oxidized to AFB_1-*exo*-8,9-epoxide in the presence of 2−3-fold molar excess of DMDO, followed by incubation for 15 min at room temperature, as previously reported, and subsequently dried with nitrogen flushing.[61] The purified unlabeled and ^{15}N-labeled oligodeoxynucleotides containing an N7-Gua alkylation site were annealed to the short complementary scaffold oligodeoxynucleotide 5′-d(TAGCGA)-3′ at an equimolar concentration, to form a partial double-stranded oligodeoxynucleotide at the site of modification. The annealing condition was 10 mmol/L sodium phosphate buffer (pH 7.5), containing 100 mmol/L NaCl and 50 μmol/L ethylenediaminetetraacetic acid disodium salt (Na_2EDTA) at 4 °C for 10 min. Next, a 6-fold molar excess of AFB_1-*exo*-8,9-epoxide (in anhydrous CH_2Cl_2) was added to the annealed oligodeoxynucleotide, and the two-phase mixture was stirred for 4 h at 4 °C to yield the AFB_1−N7-Gua-containing oligodeoxynucleotide. Subsequently, the aqueous phase of the reaction mixture was washed 3 times with CH_2Cl_2 to remove byproducts of the reaction containing AFB_1-diol. The aqueous phase with AFB_1−N7-Gua-containing oligodeoxynucleotides was separated from the unreacted oligodeoxynucleotide by HPLC with a reversed-phase C18 column at 2 mL/min flow rate and a linear, 45 min gradient of 5−15% acetonitrile in sodium phosphate buffer (2 mmol/L, pH 7.5). The elution of the separated oligodeoxynucleotides was monitored at 254 and 360 nm. Both purified unlabeled and $^{15}N_5$-labeled AFB_1−N7-Gua-containing oligodeoxynucleotides were divided in two tubes and lyophilized. One-half of the sample was dissolved in 500 μL of sodium carbonate buffer (100 mmol/L, pH 10.5) and stirred at 4 °C for 18 h for hydrolysis to form the unlabeled and $^{15}N_5$-labeled AFB_1−FapyGua adducts. The AFB_1−FapyGua-containing oligodeoxynucleotides were isolated by HPLC using a reversed-phase C18 column (Clarity C18, 250 mm × 10 mm, Phenomenex, Inc., Torrance, CA) at a flow rate of 2 mL/min with a linear, 45 min gradient of 5−15% acetonitrile in ammonium formate buffer (100 mmol/L, pH 6.8). The isolated compounds were lyophilized. The yields of the AFB_1−N7-Gua-containing oligodeoxynucleotides and AFB_1−N7-Gua-$^{15}N_5$-containing oligodeoxynucleotides were 200 and 56 μg, respectively, whereas those of AFB_1−FapyGua-containing oligodeoxynucleotides and AFB_1−FapyGua-$^{15}N_5$-containing oligodeoxynucleotides amounted to 135 and 40 μg, respectively. It should be pointed out that, because of the limited amount of the starting material of $^{15}N_5$-labeled oligodeoxynucleotides, equal initial amounts of the unlabeled and labeled oligodeoxynucleotides could not be used, leading to significant variations in the obtained final yields.

Mass Analysis by Matrix-Assisted Laser Desorption/Ionization-Time-of-Flight MS Spectrometry. Lyophilized samples of oligodeoxynucleotides were reconstituted in water and then spotted onto the matrix-assisted laser desorption/ionization (MALDI) MS plate along with the matrix 3-hydroxypicolinic acid (0.5 mol/L; saturated in 50/50 v/v water/acetonitrile) and ammonium hydrogen citrate dibasic (0.1 mol/L; 50/50 (v/v) water/acetonitrile). The spectra were collected in a reflection positive mode on a Bruker Autoflex MALDI-time-of-flight (TOF) mass spectrometer (Billerica, MA) and then evaluated using the FlexAnalysis software (Billerica, MA).

Measurements by LC−MS/MS. Mass spectral measurements and the collection of unlabeled and $^{15}N_5$-labeled *cis*-AFB_1−FapyGua, *trans*-AFB_1−FapyGua, and AFB_1−N7-Gua were performed using a Thermo TSQ Altis Triple Stage

https://doi.org/10.1021/acsomega.3c01328
ACS Omega 2023, 8, 14841−14854

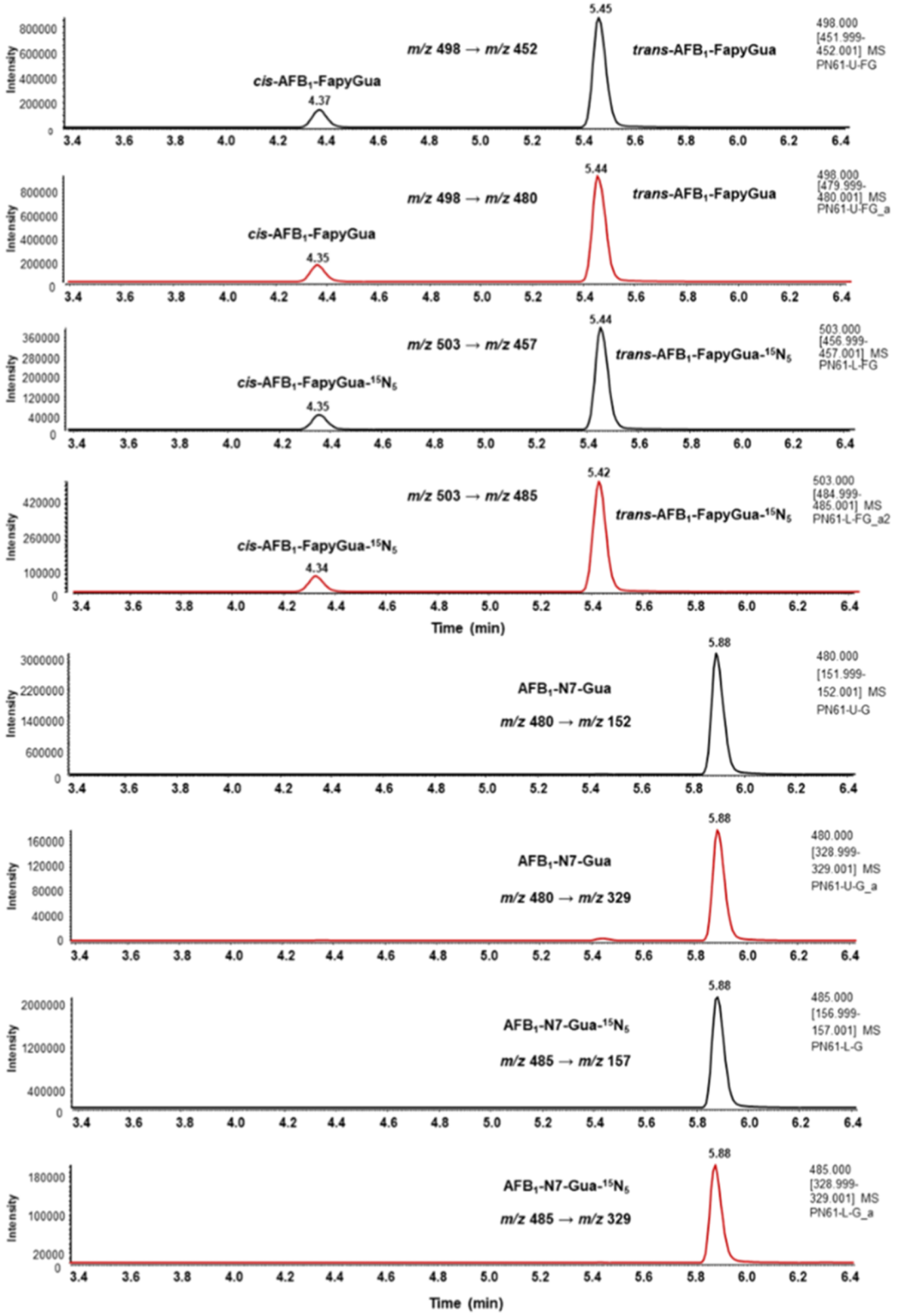

Figure 1. Ion-current profiles of the *m*/*z* transitions of *cis*-AFB_1−FapyGua, *trans*-AFB_1−FapyGua, *cis*-AFB_1−FapyGua-$^{15}N_5$, *trans*-AFB_1−FapyGua-$^{15}N_5$, AFB_1−N7-Gua, and AFB_1−N7-Gua-$^{15}N_5$ recorded during the analysis by LC−MS/MS with SRM of the hydrolyzed AFB_1−FapyGua-, AFB_1−FapyGua-$^{15}N_5$-, AFB_1−N7-Gua-, or AFB_1−N7-Gua-$^{15}N_5$-containing oligodeoxynucleotides. Each ion−current profile represents a separate analysis.

Quadrupole MS/MS system with a Vanquish Flex Quaternary ultra-high-performance liquid chromatography front-end system equipped with a diode array detector (Thermo Fisher Scientific, Waltham, MA). A Zorbax Extend C18 narrow-bore LC column (2.1 mm × 100 mm, 1.8 μm particle size) (Agilent Technologies, Wilmington, DE) with an attached Agilent Eclipse XDB-C8 guard column (2.1 mm × 12.5 mm, 5 μm particle size) was used for all separations and collections. The

https://doi.org/10.1021/acsomega.3c01328
ACS Omega 2023, 8, 14841−14854

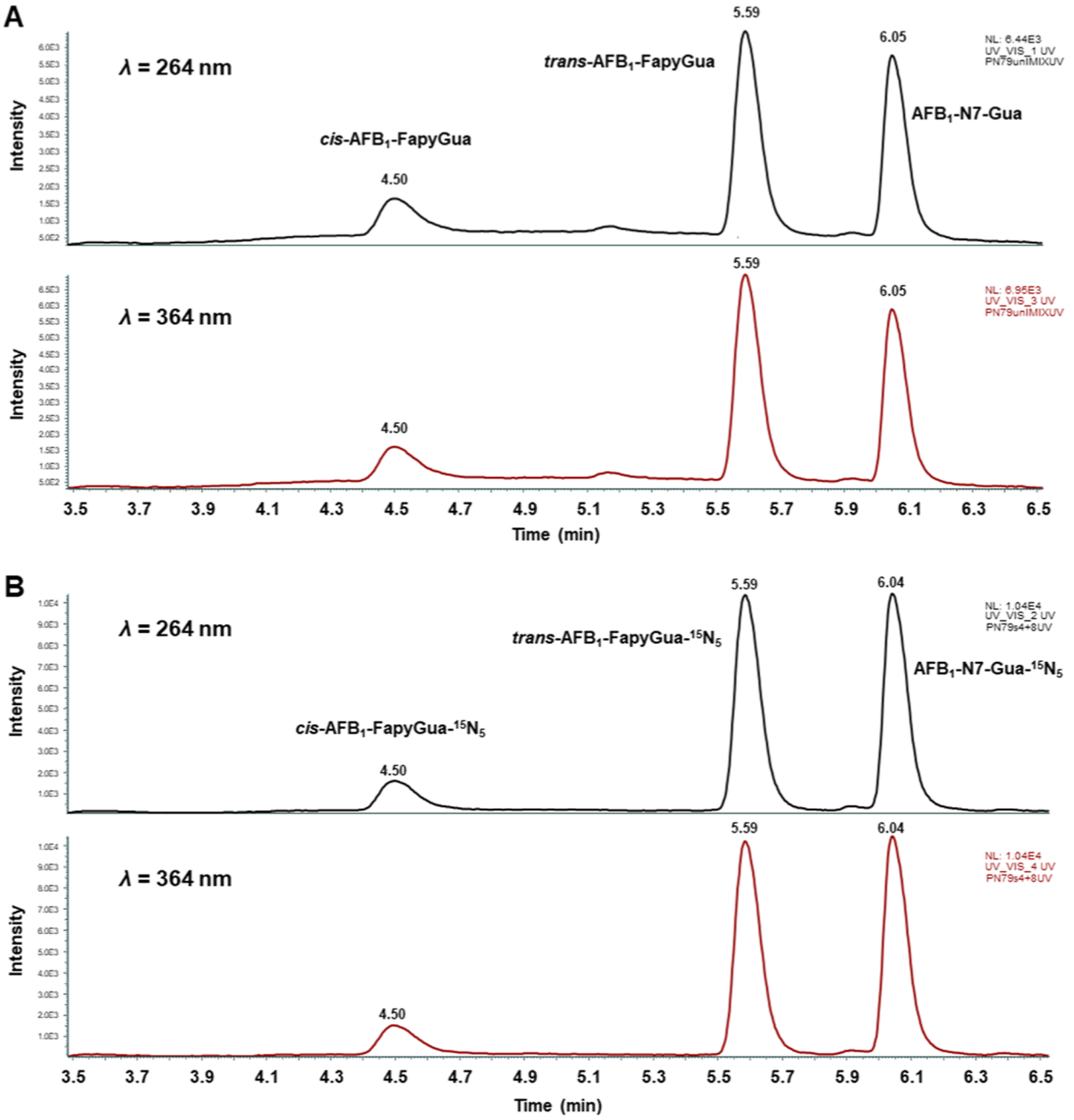

Figure 2. (A) Analysis of a mixture of hydrolyzed AFB_1−FapyGua-containing oligodeoxynucleotide and AFB_1−N7-Gua-containing oligodeoxynucleotide by LC with a diode array UV detector at 264 and 364 nm. (B) Analysis of a mixture of hydrolyzed AFB_1−FapyGua-$^{15}N_5$-containing oligodeoxynucleotide and AFB_1−N7-Gua-$^{15}N_5$-containing oligodeoxynucleotide by LC with a diode array UV detector at 264 and 364 nm.

autosampler temperature and the column temperature were kept at 6 and 40 °C, respectively. Mobile phase A was a mixture of water (98%) and acetonitrile (2%), and mobile phase B was acetonitrile, both containing 0.1% formic acid (v/v). A gradient of 8−48% of B/min in 10 min was used with a flow rate of 0.3 mL/min. After 10 min, B was increased to 90% in 0.1 min and kept at this level for 5 min and then another 15 min at 8% to equilibrate the column. The total analysis time was 30 min. The following MS/MS parameters were used: spray voltage = 3.5 kV; tube lens offsets = 89 V for Q1 and Q3; vaporizer temperature = 275 °C; ion transfer tube temperature = 350 °C; sheath gas (nitrogen) pressure = 50 (arbitrary units); auxiliary gas (nitrogen) pressure = 10 (arbitrary units); sweep gas 2 (arbitrary units); collision gas (argon) pressure = 2.67×10^{-5} Pa (2 mTorr). Selected reaction monitoring (SRM) data were acquired in the positive ionization mode at a cycle time of 0.45 s, Q1 resolution (fwhm) of 0.7, Q3 resolution (fwhm) of 1.2, and a chromatographic peak with 7 s. Total-ion chromatography data were acquired at a mass/charge (m/z) range of m/z 100 to m/z 600 with a chromatographic peak with 6 s, scan rate of 1000 Da/s, and Q1 resolution (fwhm) of 0.7. SRM scans performed with the m/z transitions: m/z 498 → 452 and m/z 498 → 480 (*cis*-AFB_1−FapyGua and *trans*-AFB_1−FapyGua), m/z 503 → 457 and m/z 503 → 485 (*cis*-AFB_1−FapyGua-$^{15}N_5$ and *trans*-AFB_1−FapyGua-$^{15}N_5$), m/z 480 → 152 and m/z 480 → 329 (AFB_1−N7-Gua), and m/z 485 → 157 and m/z 485 → 329 (AFB_1−N7-Gua-$^{15}N_5$).

https://doi.org/10.1021/acsomega.3c01328
ACS Omega 2023, 8, 14841−14854

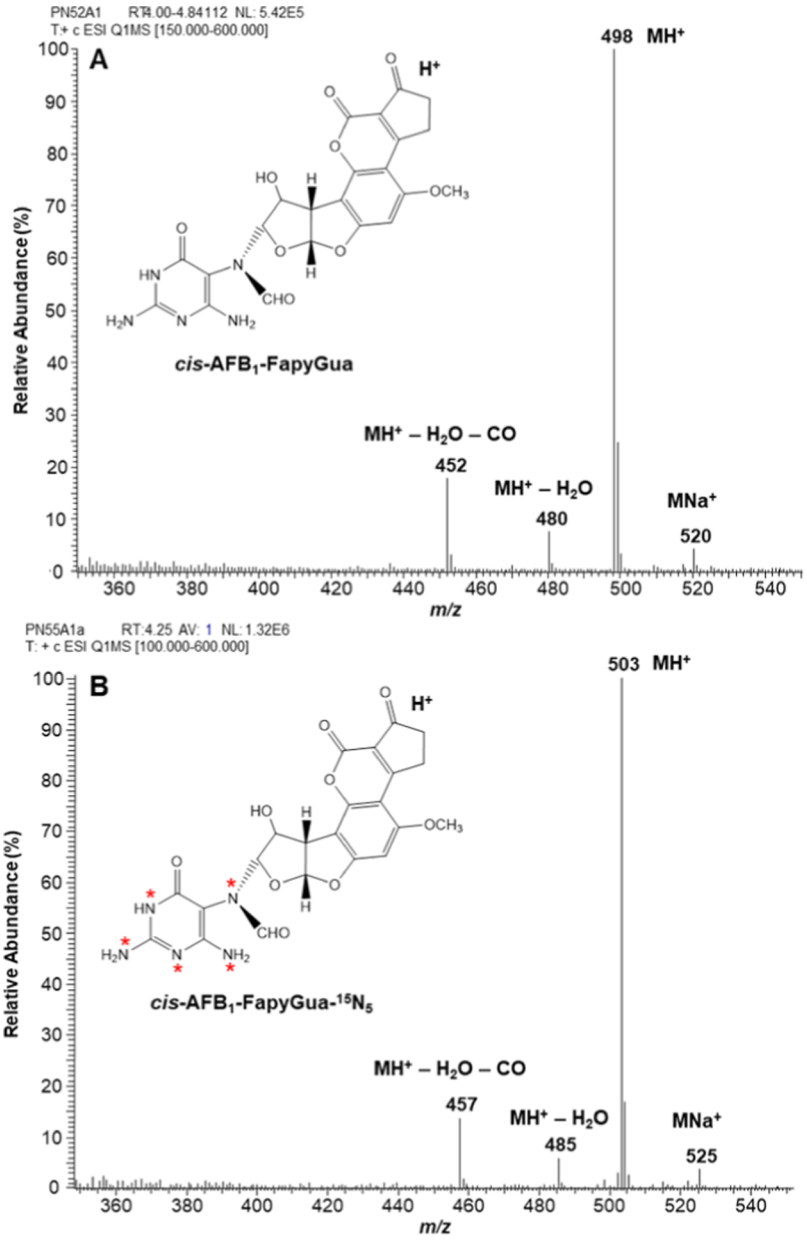

Figure 3. Full-scan mass spectra of *cis*-AFB$_1$−FapyGua (A) and *cis*-AFB$_1$−FapyGua-$^{15}N_5$ (B). The stars denote the ^{15}N-atoms.

Collection of the AFB$_1$−Gua Adducts by LC. Aliquots of oligodeoxynucleotides were dissolved in 100 μL of 0.1 mol/L HCl in Teflon-capped glass vials and then heated at 95 °C for 1 h. After cooling, the hydrolyzed samples were frozen in liquid nitrogen and lyophilized for 18 h. Dried samples were dissolved in water. Collection of the AFB$_1$−Gua adducts was performed using the analytical LC column (2.1 mm × 100 mm, 1.8 μm particle size) attached to the diode array UV detector of the LC−MS/MS instrument. The diode array UV detector was set to simultaneously monitor the effluents at 264 and 364 nm according to the UV spectra of the AFB$_1$−Gua adducts published previously.[26] The column was disconnected from the MS/MS. Six aliquots of each hydrolyzed oligodeoxynucleotide were separately injected on the LC column. After passing the UV detector, the fractions with the absorption at both 264 and 364 nm were collected manually. The collected samples were dried in a SpeedVac under vacuum.

Measurement of the UV Absorption Spectra of the Isolated AFB$_1$−Gua Adducts. The absorption spectra were recorded using a Shimadzu UV1900i UV−vis spectrophotometer (Columbia, MD).

Exposure of Mice to AFB$_1$. *Neil1*$^{-/-}$ mice that had been extensively backcrossed (19 generations) into a C57Bl6 background[57] were mated. The 6 day old pups were weighed and then given an intraperitoneal injection of freshly reconstituted AFB$_1$ in dimethyl sulfoxide (DMSO) (10 mmol/L) at a dose of 7.5 mg/kg or with DMSO only. All pups were returned to their original cages, and after 2 h, the pups were euthanized by CO_2 asphyxiation followed by decapitation. Livers were immediately harvested and frozen in either liquid nitrogen or a dry ice-ethanol slurry.

Isolation of DNA from Mouse Livers. A sample of each mouse tissue (0.2 g) was homogenized 10 times with a tissue grinder (Bullet Blender, Next Advance, Troy, NY) in 2 mL of lysis buffer (10 mmol/L Tris-HCl pH 8.2, 2 mmol/L EDTA, 0.4

https://doi.org/10.1021/acsomega.3c01328
ACS Omega 2023, 8, 14841−14854

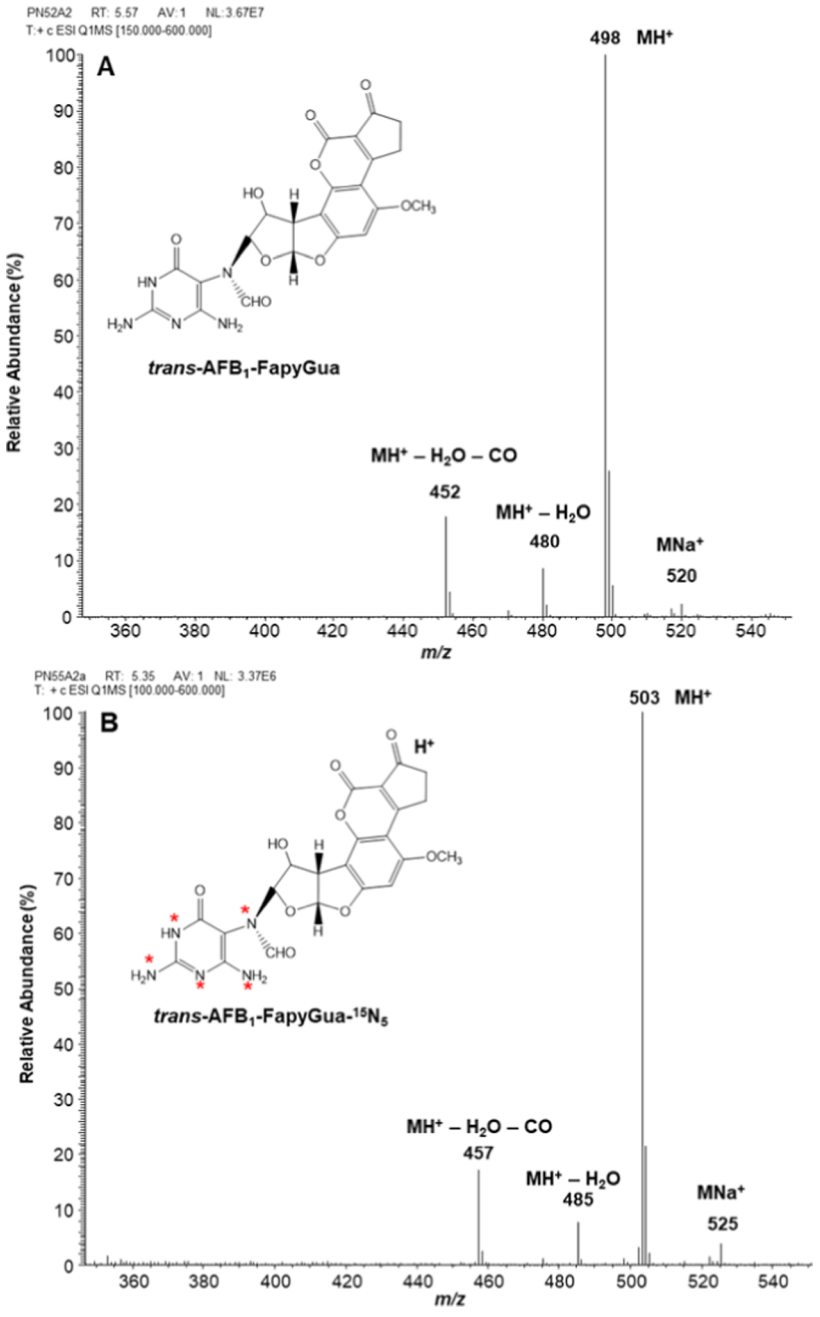

Figure 4. Full-scan mass spectra of *trans*-AFB$_1$−FapyGua (A) and *trans*-AFB$_1$−FapyGua-$^{15}N_5$ (B). The stars denote the ^{15}N-atoms.

mol/L NaCl, 1% SDS). Proteinase K (final concentration of 2 mg/mL) was added to the pellet (0.2 g tissue/2 mL lysis buffer) and incubated at 37 °C overnight. The samples were put on ice, and a 1/4 volume of saturated NaCl solution was added. The mixture was vortexed for 30 s and then incubated at 55 °C for 10 min. Precipitated peptides were removed by centrifugation at 5000 *g* for 30 min at 4 °C. The supernatant fraction was decanted into a 15 mL tube without disturbing the protein sediment. A 2.5 times volume of cold anhydrous ethanol (≥99.5%) was added to the supernatant fraction, which was then mixed gently until DNA became visible, and kept at −20 °C for 1 h until all DNA precipitated. Following centrifugation at 5000 *g* for 10 min, the supernatant fraction was removed. The DNA pellet was washed twice with 5 mL 70% ethanol and centrifuged at 5000 g for 10 min. Ethanol was decanted, with any remaining ethanol removed from the DNA pellet in a SpeedVac for 30 min. To remove any RNA, the pellet was resuspended in 1 mL TE buffer and RNase A/T1 Mix (Thermo Fisher Scientific, Waltham, MA) at a concentration of 0.2 mg/mL. The mixture was incubated at 37 °C for 1 h. DNA was precipitated and dried as described above. Each DNA sample was dissolved in water at 4 °C for 18 h. The quality and quantity of DNA were determined using an absorption spectrophotometer between 200 and 340 nm. The DNA concentration was measured using the absorbance at 260 nm (absorbance of 1 corresponds to 50 μg of double-stranded DNA). Aliquots of DNA (5 μg) were dried in a SpeedVac under vacuum and stored at 4 °C until use.

Measurements of AFB$_1$−Gua Adducts in DNA of Mouse Livers by LC−MS/MS. Aliquots (25 fmol) of each *cis*-AFB$_1$−FapyGua-$^{15}N_5$, *trans*-AFB$_1$−FapyGua-$^{15}N_5$, and AFB$_1$−N7-Gua-$^{15}N_5$ were added to three independently prepared replicates of DNA samples (5 μg each) isolated from

https://doi.org/10.1021/acsomega.3c01328
ACS Omega 2023, 8, 14841−14854

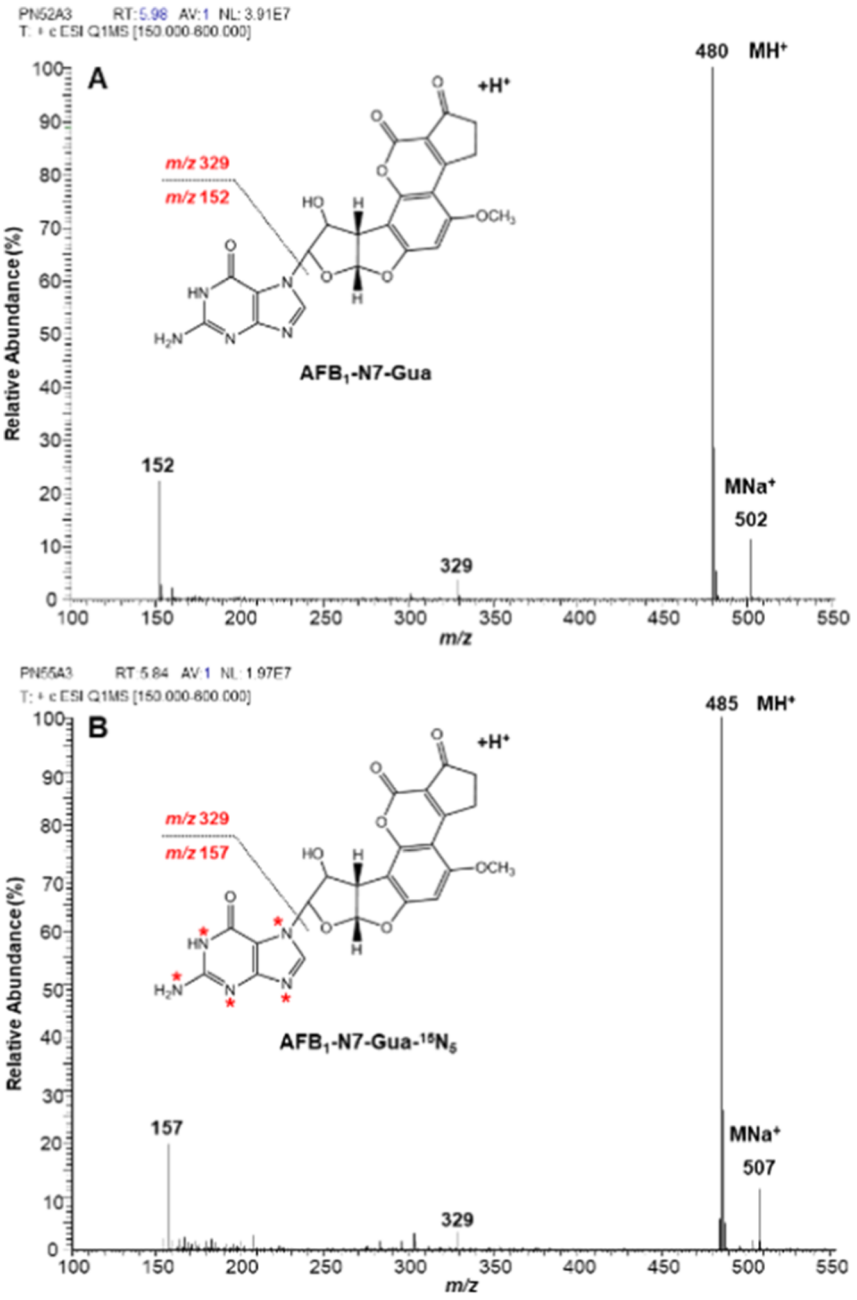

Figure 5. Full-scan mass spectra of AFB_1−N7-Gua (A) and AFB_1−N7-Gua-$^{15}N_5$ (B). The stars denote the ^{15}N-atoms.

each mouse liver DNA. The samples were dissolved in 100 μL of 0.1 mol/L HCl in Teflon-capped glass vials and then heated at 95 °C for 1 h. After cooling, the samples were frozen in liquid nitrogen and lyophilized for 18 h. The dried samples were dissolved in 60 μL of water and then filtered using Nanosep Omega tubes (Pall Life Sciences, Ann Arbor, MI). Aliquots (55 μL) of the samples were injected onto the LC column. LC−MS/MS measurements were performed as described above.

RESULTS AND DISCUSSION

The aim of this work was to synthesize, purify, and characterize the $^{15}N_5$-labeled analogues of *cis*-AFB_1−FapyGua, *trans*-AFB_1−FapyGua, and AFB_1−N7-Gua to be used as internal standards for the measurement of these adducts in biological samples such as DNA and urine by LC−MS/MS with isotope dilution. Previously, these labeled analogues were isolated and used for a variety of studies as discussed in the Introduction. In an early study, AFB_1−N7-Gua-$^{15}N_5$ was prepared by reacting AFB_1-*exo*-8,9-epoxide with uniformly ^{15}N-labeled DNA isolated from algae grown in a pure ^{15}N-environment.[56] ^{15}N-labeled DNA that was dissolved in water was treated with AFB_1-*exo*-8,9-epoxide in acetone.[23,56,61] The modified AFB_1−N7-Gua-$^{15}N_5$ was isolated and purified by HPLC from precipitated DNA after acid hydrolysis. Similarly, AFB_1−N7-Gua was obtained using calf thymus DNA treated with AFB_1-*exo*-8,9-epoxide. AFB_1−FapyGua and AFB_1−FapyGua-$^{15}N_5$ were obtained by treating AFB_1−N7-Gua and AFB_1−N7-Gua-$^{15}N_5$, respectively, with NaOH followed by isolation and purification by HPLC. In the present work, we used a different approach. We first synthesized an 11-mer oligodeoxynucleotide [5′-d(CCATC**G**CTACC)-3′] with a single $^{15}N_5$-labeled guanine at the central position. The unlabeled version of this oligodeoxynucleotide was also

https://doi.org/10.1021/acsomega.3c01328
ACS Omega 2023, 8, 14841−14854

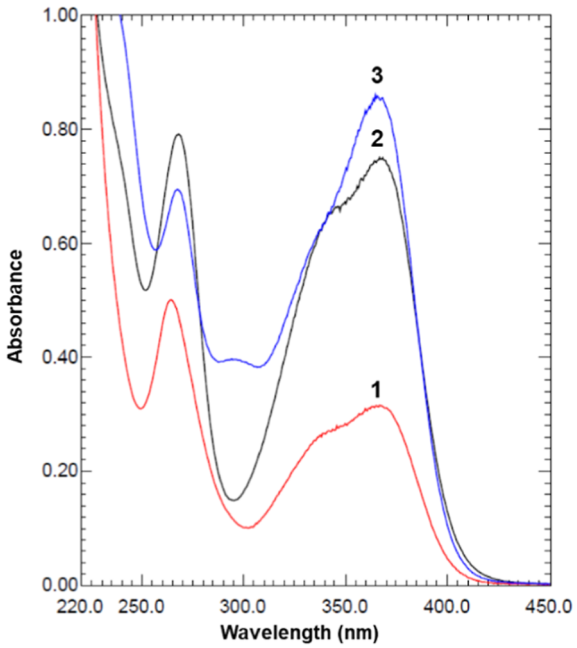

Figure 6. UV absorption spectra of *cis*-AFB_1−FapyGua (1), *trans*-AFB_1−FapyGua (2), and AFB_1−N7-Gua (3). The spectra were separately recorded and then superimposed using the Shimadzu LabSolutions UV−VIS software.

synthesized. The 11-mer was hybridized with 5′-d(TAGCGA)-3′, which placed the critical Gua in a double-stranded environment for reaction with AFB_1-*exo*-8,9-epoxide. This sequence provided the AFB_1−FapyGua-, AFB_1−FapyGua-$^{15}N_5$-, AFB_1−N7-Gua-, or AFB_1−N7-Gua-$^{15}N_5$-containing oligodeoxynucleotides, which were purified by HPLC. The corresponding unlabeled oligodeoxynucleotides were prepared in the same sequence.

MALDI-TOF MS was used to identify the synthesized oligodeoxynucleotides by measuring their masses. The measured masses for unlabeled Gua- and $^{15}N_5$-labeled Gua-containing oligodeoxynucleotides were 3236.55 Da (calc. 3237.20 Da) and 3241.71 Da (calc. 3242.20 Da), respectively. Unlabeled and $^{15}N_5$-labeled AFB_1−FapyGua-containing oligodeoxynucleotides yielded the masses 3582.34 Da (calcd 3583.48 Da) and 3587.09 Da (calcd 3588.48 Da), respectively. The mass of the $^{15}N_5$-labeled cationic AFB_1−N7-Gua-containing oligodeoxynucleotide was observed at 3570.93 Da (calcd 3570.48 Da) among the masses of AFB_1-diol-containing oligodeoxynucleotides and depurination products. However, the mass of the unlabeled cationic AFB_1−N7-Gua-containing oligodeoxynucleotide could not be determined. Only the masses of AFB_1-8,9-diol-containing oligodeoxynucleotides and depurination products were observed. Cationic AFB_1−N7-Gua-containing oligodeoxynucleotides are known to be converted to AFB_1−8,9-diol-containing oligodeoxynucleotides and/or depurinated products depending on experimental conditions.[23,25]

Next, the unlabeled and labeled AFB_1−FapyGua- and AFB_1−N7-Gua-containing oligodeoxynucleotides were hydrolyzed with HCl, lyophilized, and then analyzed by LC−MS/MS with SRM, using the known *m*/*z* transitions of AFB_1−FapyGua, AFB_1−FapyGua-$^{15}N_5$, AFB_1−N7-Gua, and AFB_1−N7-Gua-$^{15}N_5$.[19,55−57] The two major *m*/*z* transitions were used for each compound, meaning that eight analyses were performed. Figure 1 shows the ion−current profiles of the *m*/*z* transitions. For each AFB_1−FapyGua and AFB_1−FapyGua-$^{15}N_5$, two signals were observed, with the latter being approximately 4-fold more intense than the former. The signals were assigned to *cis*- and *trans*-diastereomers of each compound in agreement with the previous work.[57] AFB_1−N7-Gua and AFB_1−N7-Gua-$^{15}N_5$ yielded one signal each (Figure 1). Subsequently, the hydrolyzed oligodeoxynucleotides were analyzed using the LC with the diode array UV detector. An aliquot of the hydrolyzed AFB_1−N7-FapyGua-containing oligodeoxynucleotide and an aliquot of the hydrolyzed AFB_1−Gua-containing oligodeoxynucleotide were mixed and analyzed at 264 and 364 nm based on the previously published UV spectra of AFB_1−FapyGua and AFB_1−N7-Gua.[26] As shown in Figure 2A, three signals were observed with the use of both wavelengths at the retention times, which agreed with those in Figure 1. The analysis by the LC with UV detection of a mixture of the hydrolyzed AFB_1−FapyGua-$^{15}N_5$- and AFB_1−N7-Gua-$^{15}N_5$-containing oligodeoxynucleotides resulted in a similar profile shown in Figure 2B.

The data obtained by the mass measurements of the oligodeoxynucleotides and those shown in Figures 1 and 2 unequivocally show the successful synthesis of the AFB_1−FapyGua-, AFB_1−FapyGua-$^{15}N_5$-, AFB_1−N7-Gua-, or AFB_1−N7-Gua-$^{15}N_5$-containing oligodeoxynucleotides. The next goal was to collect the individual unlabeled and labeled AFB_1−FapyGua and AFB_1−N7-Gua adducts by LC. For this purpose, we chose to first apply the analytical column (2.1 mm × 100 mm, 1.8 μm particle size) (see Materials and Methods) that was used for the analyses to obtain the data in Figures 1 and 2. A mixture of the hydrolyzed AFB_1−N7-Gua-containing oligodeoxynucleotide and the hydrolyzed AFB_1−FapyGua-containing oligodeoxynucleotide was injected on the LC column with diode-array UV detection. The three fractions corresponding to *cis*-AFB_1−FapyGua, *trans*-AFB_1−FapyGua, and AFB_1−N7-Gua as in Figure 2 were manually collected. This was repeated six times. Similarly, *cis*-AFB_1−FapyGua-$^{15}N_5$, *trans*-AFB_1−FapyGua-$^{15}N_5$, and AFB_1−N7-Gua-$^{15}N_5$ were collected using a mixture of the hydrolyzed AFB_1−FapyGua-$^{15}N_5$-containing oligodeoxynucleotide and the hydrolyzed AFB_1−N7-Gua-$^{15}N_5$-containing oligodeoxynucleotide.

Next, the isolated compounds were analyzed by LC−MS/MS under the MS mode to individually record their total-ion mass spectra. Figures 3−5 show the total-ion mass spectra of all six compounds, with the inserts showing the corresponding structures. The protonated molecular ion (MH^+) appears as the base peak in each mass spectrum along with a low-intensity sodium adduct-ion (MNa^+). In the mass spectra of *cis*-AFB_1−FapyGua and *trans*-AFB_1−FapyGua, the ions due to the loss of H_2O from MH^+ ($MH^+ - H_2O$) and the loss of H_2O plus CO from MH^+ ($MH^+ - H_2O - CO$) are present at *m*/*z* 480 and *m*/*z* 452, respectively (Figures 3A and 4A). The masses of these ions were shifted by 5 Da to *m*/*z* 485 and *m*/*z* 457, respectively, in the mass spectra of *cis*-AFB_1−FapyGua-$^{15}N_5$ and *trans*-AFB_1−FapyGua-$^{15}N_5$ (Figures 3B and 4B). As the insert in Figure 5A shows, AFB_1−N7-Gua yielded the ions at *m*/*z* 152 and *m*/*z* 329 because of the cleavage of the bond between the purine moiety and the AFB_1 moiety. In the mass spectrum of AFB_1−N7-Gua-$^{15}N_5$ (Figure 5B), the mass of the ion at *m*/*z* 152 was shifted by 5 Da to *m*/*z* 157 due to the five ^{15}N-atoms in the purine moiety, whereas the ion at *m*/*z* 329 was present as in the figure because there was no labeled atom on the AFB_1 moiety. Partial mass spectra of AFB_1−FapyGua and AFB_1−N7-Gua isolated from rat urine,[55] and those of synthesized AFB_1−N7-Gua[19,55,56]

https://doi.org/10.1021/acsomega.3c01328
ACS Omega 2023, 8, 14841−14854

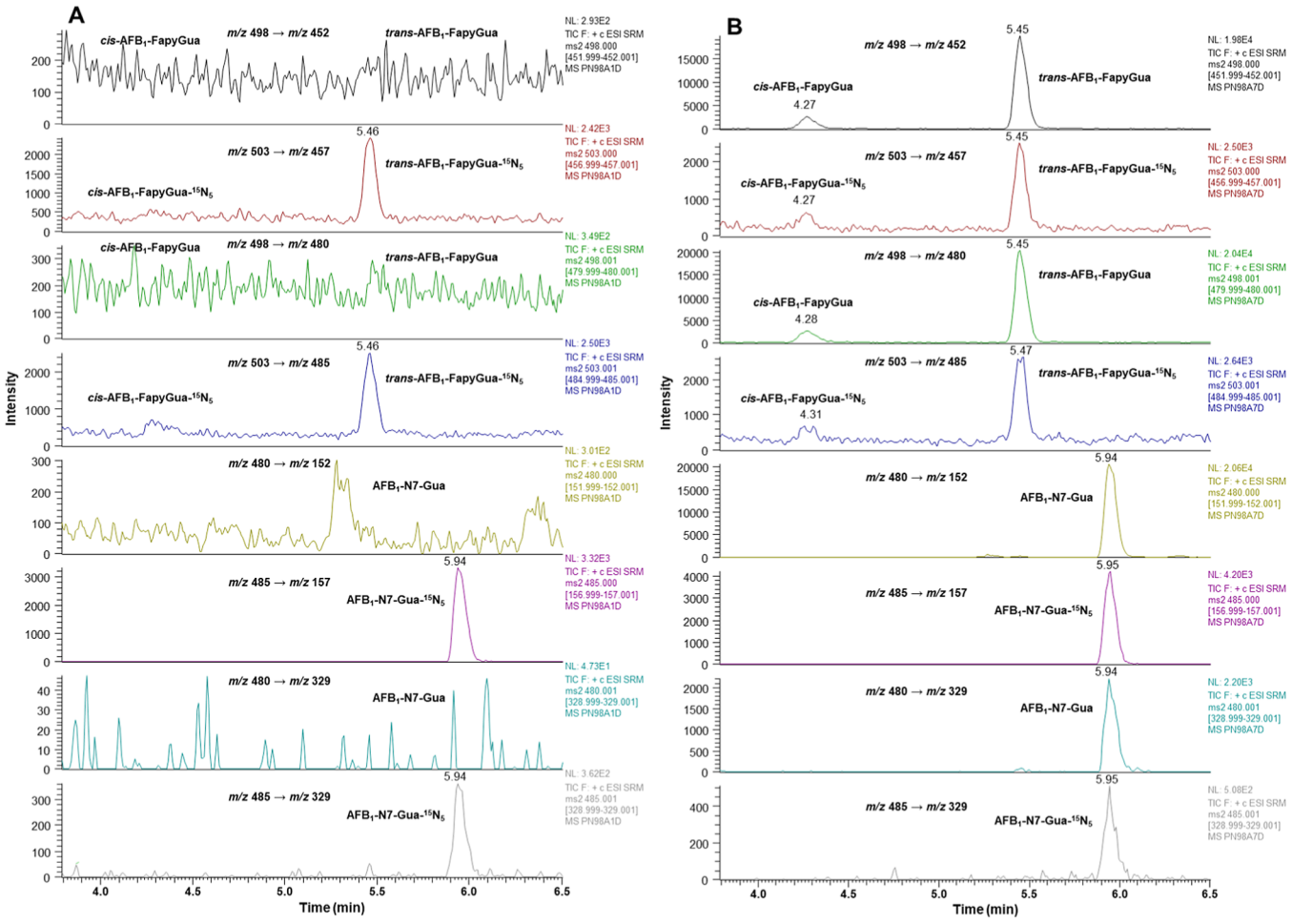

Figure 7. Ion-current profiles of the two m/z transitions of *cis*-AFB_1−FapyGua, *trans*-AFB_1−FapyGua, AFB_1−N7-Gua, *cis*-AFB_1−FapyGua-$^{15}N_5$, *trans*-AFB_1−FapyGua-$^{15}N_5$, and AFB_1−N7-Gua-$^{15}N_5$ recorded during the analysis by LC−MS/MS with the SRM of liver DNA samples (5 μg) from a control mouse (A) and from an AFB_1-treated mouse (B).

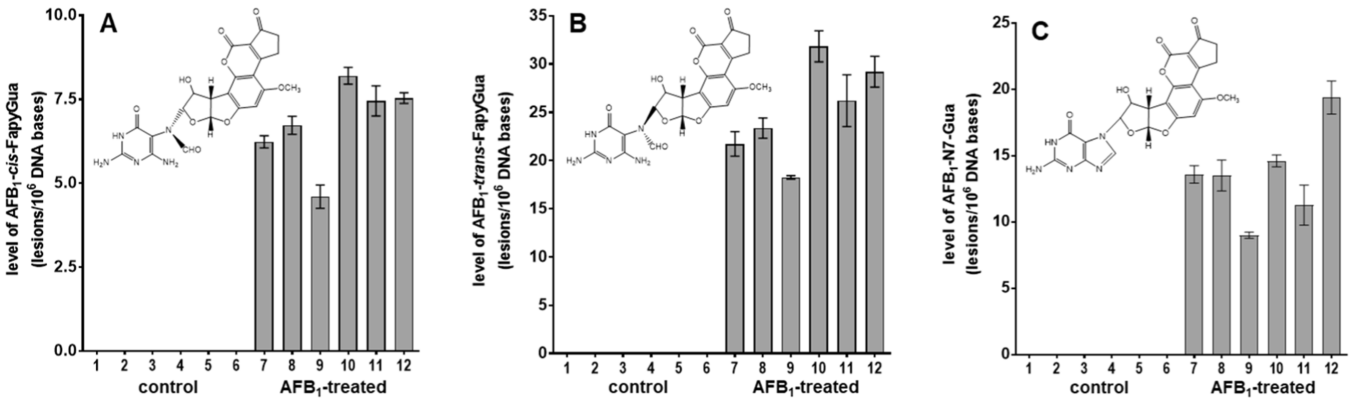

Figure 8. Levels of *cis*-AFB_1−FapyGua (A), *trans*-AFB_1−FapyGua (B), and AFB_1−N7-Gua (C) in DNA samples from livers of untreated mice (1−6) and AFB_1-treated mice (7−12). Uncertainties are standard deviations (n = 3).

and AFB_1−N7-Gua-$^{15}N_5$[56] were published previously. However, the full-scan mass spectra of all six compounds as presented in Figures 3−5 have not been published thus far. To obtain the greatest measurement sensitivity, the labeled and unlabeled compounds were individually analyzed by LC−MS/MS by varying the collision energy from 5 to 40 V to optimize this parameter. The optimum value was found to be 15 V for each compound, agreeing with the values of 15−20 V previously reported using a different instrument.[57]

Subsequently, the UV absorption spectra of the isolated compounds were recorded. Figure 6 shows the superimposed UV spectra of *cis*-AFB_1−FapyGua (1), *trans*-AFB_1−FapyGua (2), and AFB_1−N7-Gua (3). These UV absorption spectra are in excellent agreement with those published previously.[26] Two absorption maxima at 264 and 364 nm were observed in each spectrum. The labeled analogues of these compounds gave UV absorption spectra identical to those in Figure 6 (data not shown). Using the absorption abundance at 364 nm and the

https://doi.org/10.1021/acsomega.3c01328
ACS Omega 2023, 8, 14841−14854

previously reported absorption coefficient of 18,000 L mol^{-1} cm^{-1} at 364 nm,[23,26] the concentrations of the isolated compounds dissolved in 100 μL of water were calculated as follows: *cis*-AFB_1−FapyGua, 0.018 mmol/L; *trans*-AFB_1−FapyGua, 0.083 mmol/L; AFB_1−N7-Gua, 0.048 mmol/L; *cis*-AFB_1−FapyGua-$^{15}N_5$, 0.0006 mmol/L; *trans*-AFB_1−FapyGua-$^{15}N_5$, 0.0026 mmol/L; and AFB_1−N7-Gua-$^{15}N_5$, 0.022 mmol/L. The concentrations of the labeled compounds were also measured by LC−MS/MS using the unlabeled compounds as the standards. The results confirmed the values found by using the absorption spectra of the labeled compounds. Assuming that approximately 25 fmol of each labeled compound would be used for each DNA analysis, the isolated amounts of the labeled compounds would be sufficient for the LC−MS/MS analysis of at least approximately 2000 DNA samples. This means that the simple use of an analytical column instead of a semi-preparative column for the collection of *cis*-AFB_1−FapyGua-$^{15}N_5$, *trans*-AFB_1−FapyGua-$^{15}N_5$, and AFB_1−N7-Gua-$^{15}N_5$, as was done in this work, would suffice for the purpose of isolation and purification of these compounds.

To validate the use of the isolated $^{15}N_5$-labeled internal standards, DNA was isolated from the livers of mice treated with DMSO or with AFB_1. We used 5 μg aliquots of DNA samples, which were supplemented with 25 fmol aliquots of the internal standards. The samples were hydrolyzed and then analyzed by LC−MS/MS with SRM. As examples, Figure 7A,B shows the ion−current profiles of the two *m*/*z* transitions of *cis*-AFB_1−FapyGua (*m*/*z* 498 → 452 and *m*/*z* 498 → 480), *cis*-AFB_1−FapyGua-$^{15}N_5$ (*m*/*z* 503 → 457 and *m*/*z* 503 → 485), *trans*-AFB_1−FapyGua (*m*/*z* 498 → 452 and *m*/*z* 498 → 480), *trans*-AFB_1−FapyGua-$^{15}N_5$ (*m*/*z* 503 → 457 and *m*/*z* 503 → 485), AFB_1−N7-Gua (*m*/*z* 480 → 152 and *m*/*z* 480 → 329), and AFB_1−N7-Gua-$^{15}N_5$ (*m*/*z* 485 → 157 and *m*/*z* 485 → 329), which were simultaneously recorded during the analyses of 5 μg aliquots of DNA samples from livers of mice treated with DMSO and AFB_1, respectively. The simultaneous monitoring of the two *m*/*z* transitions of each compound and their ^{15}N-labeled analogues validates the identification and quantification. As Figure 7B shows, intense signals of the *m*/*z* transitions of *cis*-AFB_1−FapyGua, *trans*-AFB_1−FapyGua, and AFB_1−N7-Gua were observed in liver DNA samples from AFB_1-treated mice when compared to DNA samples from control mice (Figure 7A), unequivocally identifying the presence of these adducts in liver DNA of AFB_1-treated mice. *Cis*-AFB_1−FapyGua, *trans*-AFB_1−FapyGua, and AFB_1−N7-Gua were not detectable in DNA samples from livers of 6 mice treated with DMSO only, as shown in Figure 7A. The individual analysis of *cis*-AFB_1−FapyGua-$^{15}N_5$, *trans*-AFB_1−FapyGua-$^{15}N_5$, and AFB_1−N7-Gua-$^{15}N_5$ at the levels of 25 fmol showed no detectable background levels of their unlabeled analogues, either. Figure 8A−C shows the measured levels of *cis*-AFB_1−FapyGua, *trans*-AFB_1−FapyGua, and AFB_1−N7-Gua, respectively, in DNA samples isolated from the livers of 6 AFB_1-treated mice. These results show that all three AFB_1−Gua adducts can be readily detected and quantified in 5 μg aliquots of DNA samples under the experimental conditions used in this work. This amount corresponds to the approximate recovery amount of DNA from 5 mg of human liver biopsy samples as previously reported.[62]

The limit of quantification (LOQ) for AFB_1−N7-Gua was determined to be 0.04 fmol injected on a column. This value agrees with the previously published values of 0.042[56] and 0.036 fmol.[56,57] However, the LOQ values for *cis*-AFB_1−FapyGua and *trans*-AFB_1−FapyGua were 0.3 and 0.15 fmol injected on the column, respectively, which are approximately 8 and 4 times higher than the values of 0.036 fmol obtained using a different LC−MS/MS instrument.[57] The reason for this discrepancy is not known. The LOQ levels of 0.3, 0.15, and 0.04 fmol correspond to approximately 2 *cis*-AFB_1−FapyGua lesions/10^8 DNA bases, 1 *trans*-AFB_1−FapyGua lesions/10^8 DNA bases, and 2.6 AFB_1−N7-Gua lesions/10^9 DNA bases, respectively. This suggests that these lesions can be measured at least at these levels in DNA by the methodology described in this work.

In conclusion, we prepared, isolated, and fully characterized the $^{15}N_5$-labeled analogues of *cis*-AFB_1−FapyGua, *trans*-AFB_1−FapyGua, and AFB_1−N7-Gua to be used as internal standards for the MS measurements of these adducts in biological samples such as DNA and urine. We also demonstrated the application of these $^{15}N_5$-labeled internal standards to the measurement of these adducts in DNA of livers of AFB_1-treated mice in vivo using as low as 5 μg of DNA. This work may contribute to basic and applied research and to prevention, clinical, and intervention trials concerning the role of AFB_1 toxicity in hepatocarcinogenesis.

AUTHOR INFORMATION

Corresponding Authors

Pawel Jaruga − *Biomolecular Measurement Division, National Institute of Standards and Technology, Gaithersburg, Maryland 20899, United States*; Email: pawel.jaruga@nist.gov

Miral Dizdaroglu − *Biomolecular Measurement Division, National Institute of Standards and Technology, Gaithersburg, Maryland 20899, United States*; orcid.org/0000-0003-0283-1695; Email: miral.dizdar@nist.gov

Authors

Rachana Tomar − *Department of Chemistry, Vanderbilt Ingram Cancer Center, Vanderbilt University, Nashville, Tennessee 37235, United States*

Melis Kant − *Biomolecular Measurement Division, National Institute of Standards and Technology, Gaithersburg, Maryland 20899, United States*

Vladimir Vartanian − *Oregon Institute of Occupational Health Sciences, Oregon Health & Science University, Portland, Oregon 97239, United States*

Benjamin Sexton − *Department of Chemistry, Vanderbilt Ingram Cancer Center, Vanderbilt University, Nashville, Tennessee 37235, United States*

Carmelo J. Rizzo − *Department of Chemistry, Vanderbilt Ingram Cancer Center, Vanderbilt University, Nashville, Tennessee 37235, United States*; orcid.org/0000-0001-9005-611X

Robert J. Turesky − *Masonic Cancer Center, University of Minnesota, Minneapolis, Minnesota 55455, United States*; orcid.org/0000-0001-7355-9903

Michael P. Stone − *Department of Chemistry, Vanderbilt Ingram Cancer Center, Vanderbilt University, Nashville, Tennessee 37235, United States*; orcid.org/0000-0002-0922-0216

R. Stephen Lloyd − *Oregon Institute of Occupational Health Sciences, Oregon Health & Science University, Portland, Oregon 97239, United States*; orcid.org/0000-0001-7273-372X

Complete contact information is available at: https://pubs.acs.org/10.1021/acsomega.3c01328

https://doi.org/10.1021/acsomega.3c01328
ACS Omega 2023, 8, 14841−14854

Funding

This work was partially supported by the following sources: National Institute of Standards and Technology (P.J., M.K., and M.D.) and National Institutes of Health (NIH) grants R01 CA-55678, R01 ES-029357, and P01 CA-160032 (M.P.S., C.J.R, R.J.T., and R.S.L.). R.S.L. acknowledges support from the National Institute of Environmental Health Sciences (R01 ES-031086) and from the Oregon Institute of Occupational Health Sciences at Oregon Health & Science University via funds from the Division of Consumer and Business Services of the State of Oregon (ORS 656.630). The Vanderbilt-Ingram Cancer Center was funded by NIH grant P30 CA-068485.

Notes

The authors declare no competing financial interest.

■ ACKNOWLEDGMENTS

Certain equipment, instruments, software, or materials, commercial or non-commercial, are identified in this paper in order to specify the experimental procedure adequately. Such identification is not intended to imply recommendation or endorsement of any product or service by NIST, nor is it intended to imply that the materials or equipment identified are necessarily the best available for the purpose. This work with the Project no. MML-16-0016 and with the Research Collaboration Agreement no. RCA-23-001 between Oregon Health & Science University (OHSU) and NIST was reviewed and approved by the Office of Technology Transfer of OHSU and the Technology Partnership Office of NIST. We thank Dr. Michelle Reyzer at Vanderbilt Mass Spectrometry facility for her assistance in the measurements with MALDI-TOF mass spectrometry. We thank Dr. John Groopman of Johns Hopkins University, Bloomberg School of Public Health, Baltimore, Maryland, for very helpful discussions.

■ REFERENCES

(1) Blonski, W.; Kotlyar, D. S.; Forde, K. A. Non-viral causes of hepatocellular carcinoma. *World J. Gastroenterol.* **2010**, *16*, 3603−3615.
(2) Kensler, T. W.; Roebuck, B. D.; Wogan, G. N.; Groopman, J. D. Aflatoxin: a 50-year odyssey of mechanistic and translational toxicology. *Toxicol. Sci.* **2011**, *120*, S28−S48.
(3) Kew, M. C. Aflatoxins as a cause of hepatocellular carcinoma. *J. Gastrointestin. Liver Dis.* **2013**, *22*, 305−310.
(4) McCullough, A. K.; Lloyd, R. S. Mechanisms underlying aflatoxin-associated mutagenesis - Implications in carcinogenesis. *DNA Repair* **2019**, *77*, 76−86.
(5) Smith, J. W.; Groopman, J. D. Translating DNA adduct knowledge to human prevential trials. In *DNA Damage, DNA Repair and Disease*; Dizdaroglu, M., Lloyd, R. S., Eds.; Royal Society of Chemistry: Cambridge, United Kingdom, 2021; pp 361-387.
(6) Fedeles, B. I.; Essigmann, J. M. Mutational spectra provide insight into the mechanisms bridging DNA damage to genetic disease. In *DNA Damage, DNA Repair and Disease*; Dizdaroglu, M., Lloyd, R. S., Eds.; Royal Society of Chemistry: Cambridge, United Kingdom, 2021; pp 214−253.
(7) Ayres, J. L.; Lee, D. J.; Wales, J. H.; Sinnhuber, R. O. Aflatoxin structure and hepatocarcinogenicity in rainbow trout (Salmo gairdneri). *J. Natl. Cancer Inst.* **1971**, *46*, 561−564.
(8) Wogan, G. N.; Edwards, G. S.; Newberne, P. M. Structure-activity relationships in toxicity and carcinogenicity of aflatoxins and analogs. *Cancer Res.* **1971**, *31*, 1936−1942.
(9) Groopman, J. D.; Kensler, T. W.; Wu, F. Food Safety (a) Mycotoxins: Occurrence and Toxic Effects. In *Encyclopedia of Human Nutrition*; Caballero, B., Allen, L., Prentice, A., Eds.; Elsevier, 2011; pp 337−345.
(10) Wogan, G. N.; Kensler, T. W.; Groopman, J. D. Present and future directions of translational research on aflatoxin and hepatocellular carcinoma. A review. *Food Addit. Contam., Part A* **2012**, *29*, 249−257.
(11) Wu, F.; Groopman, J. D.; Pestka, J. J. Public health impacts of foodborne mycotoxins. *Annu. Rev. Food Sci. Technol.* **2014**, *5*, 351−372.
(12) Kew, M. C. Synergistic interaction between aflatoxin B1 and hepatitis B virus in hepatocarcinogenesis. *Liver Int.* **2003**, *23*, 405−409.
(13) Groopman, J. D.; Johnson, D.; Kensler, T. W. Aflatoxin and hepatitis B virus biomarkers: a paradigm for complex environmental exposures and cancer risk. *Cancer Biomarkers* **2005**, *1*, 5−14.
(14) Groopman, J. D.; Kensler, T. W. Role of metabolism and viruses in aflatoxin-induced liver cancer. *Toxicol. Appl. Pharmacol.* **2005**, *206*, 131−137.
(15) Donnelly, P. J.; Devereux, T. R.; Foley, J. F.; Maronpot, R. R.; Anderson, M. W.; Massey, T. E. Activation of K-ras in aflatoxin B_1-induced lung tumors from AC3F1 (A/J×C3H/HeJ) mice. *Carcinogenesis* **1996**, *17*, 1735−1740.
(16) Donnelly, P. J.; Stewart, R. K.; Ali, S. L.; Conlan, A. A.; Reid, K. R.; Petsikas, D.; Massey, T. E. Biotransformation of aflatoxin B1 in human lung. *Carcinogenesis* **1996**, *17*, 2487−2494.
(17) Massey, T. E.; Smith, G. B.; Tam, A. S. Mechanisms of aflatoxin B1 lung tumorigenesis. *Exp. Lung Res.* **2000**, *26*, 673−683.
(18) Kamdem, L. K.; Meineke, I.; Godtel-Armbrust, U.; Brockmoller, J.; Wojnowski, L. Dominant contribution of P450 3A4 to the hepatic carcinogenic activation of aflatoxin B1. *Chem. Res. Toxicol.* **2006**, *19*, 577−586.
(19) Essigmann, J. M.; Croy, R. G.; Nadzan, A. M.; Busby, W. F., Jr.; Reinhold, V. N.; Buchi, G.; Wogan, G. N. Structural identification of the major DNA adduct formed by aflatoxin B1 in vitro. *Proc. Natl. Acad. Sci. U.S.A.* **1977**, *74*, 1870−1874.
(20) Martin, C. N.; Garner, R. C. Aflatoxin B-oxide generated by chemical or enzymic oxidation of aflatoxin B1 causes guanine substitution in nucleic acids. *Nature* **1977**, *267*, 863−865.
(21) Croy, R. G.; Essigmann, J. M.; Reinhold, V. N.; Wogan, G. N. Identification of the principal aflatoxin B1-DNA adduct formed in vivo in rat liver. *Proc. Natl. Acad. Sci. U.S.A.* **1978**, *75*, 1745−1749.
(22) Croy, R. G.; Wogan, G. N. Temporal patterns of covalent DNA adducts in rat liver after single and multiple doses of aflatoxin B1. *Cancer Res.* **1981**, *41*, 197−203.
(23) Groopman, J. D.; Croy, R. G.; Wogan, G. N. In vitro reactions of aflatoxin B1-adducted DNA. *Proc. Natl. Acad. Sci. U.S.A.* **1981**, *78*, 5445−5449.
(24) Brown, K. L.; Deng, J. Z.; Iyer, R. S.; Iyer, L. G.; Voehler, M. W.; Stone, M. P.; Harris, C. M.; Harris, T. M. Unraveling the aflatoxin-FAPY conundrum: structural basis for differential replicative processing of isomeric forms of the formamidopyrimidine-type DNA adduct of aflatoxin B1. *J. Am. Chem. Soc.* **2006**, *128*, 15188−15199.
(25) Essigmann, J. M.; Green, C. L.; Croy, R. G.; Fowler, K. W.; Buchi, G. H.; Wogan, G. N. Interactions of aflatoxin B1 and alkylating agents with DNA: structural and functional studies. *Cold Spring Harbor Symp. Quant. Biol.* **1983**, *47*, 327−337.
(26) Lin, J. K.; Miller, J. A.; Miller, E. C. 2,3-Dihydro-2-(guan-7-yl)-3-hydroxy-aflatoxin B1, a major acid hydrolysis product of aflatoxin B1-DNA or -ribosomal RNA adducts formed in hepatic microsome-mediated reactions and in rat liver in vivo. *Cancer Res.* **1977**, *37*, 4430−4438.
(27) Hertzog, P. J.; Smith, J. R.; Garner, R. C. Characterisation of the imidazole ring-opened forms of trans-8,9-di-hydro-8-(7-guanyl)9-hydroxy aflatoxin B_1. *Carcinogenesis* **1982**, *3*, 723−725.
(28) Bailey, E. A.; Iyer, R. S.; Stone, M. P.; Harris, T. M.; Essigmann, J. M. Mutational properties of the primary aflatoxin B1-DNA adduct. *Proc. Natl. Acad. Sci. U.S.A.* **1996**, *93*, 1535−1539.
(29) Smela, M. E.; Currier, S. S.; Bailey, E. A.; Essigmann, J. M. The chemistry and biology of aflatoxin B(1): from mutational spectrometry to carcinogenesis. *Carcinogenesis* **2001**, *22*, 535−545.
(30) Smela, M. E.; Hamm, M. L.; Henderson, P. T.; Harris, C. M.; Harris, T. M.; Essigmann, J. M. The aflatoxin B(1) formamidopyrimidine adduct plays a major role in causing the types of mutations

https://doi.org/10.1021/acsomega.3c01328
ACS Omega 2023, 8, 14841−14854

observed in human hepatocellular carcinoma. *Proc. Natl. Acad. Sci. U.S.A.* **2002**, *99*, 6655−6660.
(31) Lin, Y. C.; Li, L.; Makarova, A. V.; Burgers, P. M.; Stone, M. P.; Lloyd, R. S. Error-prone replication bypass of the primary aflatoxin B1 DNA adduct, AFB1-N7-Gua. *J. Biol. Chem.* **2014**, *289*, 18497−18506.
(32) Lin, Y. C.; Li, L.; Makarova, A. V.; Burgers, P. M.; Stone, M. P.; Lloyd, R. S. Molecular basis of aflatoxin-induced mutagenesis-role of the aflatoxin B1-formamidopyrimidine adduct. *Carcinogenesis* **2014**, *35*, 1461−1468.
(33) Fedeles, B. I.; Essigmann, J. M. Impact of DNA lesion repair, replication and formation on the mutational spectra of environmental carcinogens: Aflatoxin B1 as a case study. *DNA Repair* **2018**, *71*, 12−22.
(34) Mao, H.; Deng, Z.; Wang, F.; Harris, T. M.; Stone, M. P. An intercalated and thermally stable FAPY adduct of aflatoxin B1 in a DNA duplex: structural refinement from 1H NMR. *Biochemistry* **1998**, *37*, 4374−4387.
(35) Brown, K. L.; Voehler, M. W.; Magee, S. M.; Harris, C. M.; Harris, T. M.; Stone, M. P. Structural perturbations induced by the alpha-anomer of the aflatoxin B(1) formamidopyrimidine adduct in duplex and single-strand DNA. *J. Am. Chem. Soc.* **2009**, *131*, 16096−16107.
(36) Oleykowski, C. A.; Mayernik, J. A.; Lim, S. E.; Groopman, J. D.; Grossman, L.; Wogan, G. N.; Yeung, A. T. Repair of aflatoxin B1 DNA adducts by the UvrABC endonuclease of Escherichia coli. *J. Biol. Chem.* **1993**, *268*, 7990−8002.
(37) Alekseyev, Y. O.; Hamm, M. L.; Essigmann, J. M. Aflatoxin B1 formamidopyrimidine adducts are preferentially repaired by the nucleotide excision repair pathway in vivo. *Carcinogenesis* **2004**, *25*, 1045−1051.
(38) Chetsanga, C. J.; Frenette, G. P. Excision of Aflatoxin B1-Imidazole Ring Opened Guanine Adducts from DNA by Formamidopyrimidine-DNA Glycosylase. *Carcinogenesis* **1983**, *4*, 997−1000.
(39) Hazra, T. K.; Izumi, T.; Boldogh, I.; Imhoff, B.; Kow, Y. W.; Jaruga, P.; Dizdaroglu, M.; Mitra, S. Identification and characterization of a human DNA glycosylase for repair of modified bases in oxidatively damaged DNA. *Proc. Natl. Acad. Sci. U.S.A.* **2002**, *99*, 3523−3528.
(40) Dizdaroglu, M.; Coskun, E.; Jaruga, P. Repair of oxidatively induced DNA damage by DNA glycosylases: Mechanisms of action, substrate specificities and excision kinetics. *Mutat. Res. Rev. Mutat. Res.* **2017**, *771*, 99−127.
(41) Vartanian, V.; Minko, I. G.; Chawanthayatham, S.; Egner, P. A.; Lin, Y. C.; Earley, L. F.; Makar, R.; Eng, J. R.; Camp, M. T.; Li, L.; Stone, M. P.; Lasarev, M. R.; Groopman, J. D.; Croy, R. G.; Essigmann, J. M.; McCullough, A. K.; Lloyd, R. S. NEIL1 protects against aflatoxin-induced hepatocellular carcinoma in mice. *Proc. Natl. Acad. Sci. U.S.A.* **2017**, *114*, 4207−4212.
(42) Minko, I. G.; Vartanian, V. L.; Tozaki, N. N.; Linde, O. K.; Jaruga, P.; Coskun, S. H.; Coskun, E.; Qu, C. F.; He, H.; Xu, C. G.; Chen, T. Y.; Song, Q.; Jiao, Y. C.; Stone, M. P.; Egli, M.; Dizdaroglu, M.; McCullough, A. K.; Lloyd, R. S. Characterization of rare NEIL1 variants found in East Asian populations. *DNA Repair* **2019**, *79*, 32−39.
(43) Minko, I. G.; Vartanian, V. L.; Tozaki, N. N.; Coskun, E.; Coskun, S. H.; Jaruga, P.; Yeo, J.; David, S. S.; Stone, M. P.; Egli, M.; Dizdaroglu, M.; McCullough, A. K.; Lloyd, R. S. Recognition of DNA adducts by edited and unedited forms of DNA glycosylase NEIL1. *DNA Repair* **2020**, *85*, 102741.
(44) Tomar, R.; Minko, I. G.; Kellum, A. H., Jr.; Voehler, M. W.; Stone, M. P.; McCullough, A. K.; Lloyd, R. S. DNA sequence modulates the efficiency of NEIL1-catalyzed excision of the aflatoxin B1-Induced formamidopyrimidine guanine adduct. *Chem. Res. Toxicol.* **2021**, *34*, 901−911.
(45) Roy, L. M.; Jaruga, P.; Wood, T. G.; McCullough, A. K.; Dizdaroglu, M.; Lloyd, R. S. Human polymorphic variants of the NEIL1 DNA glycosylase. *J. Biol. Chem.* **2007**, *282*, 15790−15798.
(46) Prakash, A.; Carroll, B. L.; Sweasy, J. B.; Wallace, S. S.; Doublie, S. Genome and cancer single nucleotide polymorphisms of the human NEIL1 DNA glycosylase: activity, structure, and the effect of editing. *DNA Repair* **2014**, *14*, 17−26.
(47) Galick, H. A.; Marsden, C. G.; Kathe, S.; Dragon, J. A.; Volk, L.; Nemec, A. A.; Wallace, S. S.; Prakash, A.; Doublie, S.; Sweasy, J. B. The NEIL1 G83D germline DNA glycosylase variant induces genomic instability and cellular transformation. *Oncotarget* **2017**, *8*, 85883−85895.
(48) Shepherd, M. J.; Gilbert, J. An investigation of HPLC post-column iodination conditions for the enhancement of aflatoxin B1 fluorescence. *Food Addit. Contam.* **1984**, *1*, 325−335.
(49) Groopman, J. D.; Donahue, P. R.; Zhu, J. Q.; Chen, J. S.; Wogan, G. N. Aflatoxin Metabolism in Humans - Detection of Metabolites and Nucleic-Acid Adducts in Urine by Affinity-Chromatography. *Proc. Natl. Acad. Sci. U.S.A.* **1985**, *82*, 6492−6496.
(50) Harris, C. C.; LaVeck, G.; Groopman, J.; Wilson, V. L.; Mann, D. Measurement of aflatoxin B1, its metabolites, and DNA adducts by synchronous fluorescence spectrophotometry. *Cancer Res.* **1986**, *46*, 3249−3253.
(51) Groopman, J. D.; Hall, A. J.; Whittle, H.; Hudson, G. J.; Wogan, G. N.; Montesano, R.; Wild, C. P. Molecular dosimetry of aflatoxin-N7-guanine in human urine obtained in The Gambia, West Africa. *Cancer Epidemiol. Biomark. Prev.* **1992**, *1*, 221−227.
(52) Groopman, J. D.; Zhu, J. Q.; Donahue, P. R.; Pikul, A.; Zhang, L. S.; Chen, J. S.; Wogan, G. N. Molecular dosimetry of urinary aflatoxin-DNA adducts in people living in Guangxi Autonomous Region, People's Republic of China. *Cancer Res.* **1992**, *52*, 45−52.
(53) Groopman, J. D.; Wild, C. P.; Hasler, J.; Junshi, C.; Wogan, G. N.; Kensler, T. W. Molecular epidemiology of aflatoxin exposures: validation of aflatoxin-N7-guanine levels in urine as a biomarker in experimental rat models and humans. *Environ. Health Perspect.* **1993**, *99*, 107−113.
(54) Wang, J. S.; Shen, X.; He, X.; Zhu, Y. R.; Zhang, B. C.; Wang, J. B.; Qian, G. S.; Kuang, S. Y.; Zarba, A.; Egner, P. A.; Jacobson, L. P.; Munoz, A.; Helzlsouer, K. J.; Groopman, J. D.; Kensler, T. W. Protective alterations in phase 1 and 2 metabolism of aflatoxin B1 by oltipraz in residents of Qidong, People's Republic of China. *J. Natl. Cancer Inst.* **1999**, *91*, 347−354.
(55) Walton, M.; Egner, P.; Scholl, P. F.; Walker, J.; Kensler, T. W.; Groopman, J. D. Liquid chromatography electrospray-mass spectrometry of urinary aflatoxin biomarkers: characterization and application to dosimetry and chemoprevention in rats. *Chem. Res. Toxicol.* **2001**, *14*, 919−926.
(56) Egner, P. A.; Groopman, J. D.; Wang, J. S.; Kensler, T. W.; Friesen, M. D. Quantification of aflatoxin-B1-N7-Guanine in human urine by high-performance liquid chromatography and isotope dilution tandem mass spectrometry. *Chem. Res. Toxicol.* **2006**, *19*, 1191−1195.
(57) Coskun, E.; Jaruga, P.; Vartanian, V.; Erdem, O.; Egner, P. A.; Groopman, J. D.; Lloyd, R. S.; Dizdaroglu, M. Aflatoxin-Guanine DNA Adducts and Oxidatively Induced DNA Damage in Aflatoxin-Treated Mice in Vivo as Measured by Liquid Chromatography-Tandem Mass Spectrometry with Isotope Dilution. *Chem. Res. Toxicol.* **2019**, *32*, 80−89.
(58) Elmquist, C. E.; Stover, J. S.; Wang, Z.; Rizzo, C. J. Site-specific synthesis and properties of oligonucleotides containing C8-deoxyguanosine adducts of the dietary mutagen IQ. *J. Am. Chem. Soc.* **2004**, *126*, 11189−11201.
(59) Li, L.; Brown, K. L.; Ma, R.; Stone, M. P. DNA Sequence Modulates Geometrical Isomerism of the trans-8,9- Dihydro-8-(2,6-diamino-4-oxo-3,4-dihydropyrimid-5-yl-formamido)- 9-hydroxy Aflatoxin B1 Adduct. *Chem. Res. Toxicol.* **2015**, *28*, 225−237.
(60) Adam, W.; Chan, Y. Y.; Cremer, D.; Gauss, J.; Scheutzow, D.; Schindler, M. Spectral and Chemical-Properties of Dimethyldioxirane as Determined by Experiment and Abinitio Calculations. *J. Org. Chem.* **1987**, *52*, 2800−2803.
(61) Baertschi, S. W.; Raney, K. D.; Stone, M. P.; Harris, T. M. Preparation of the 8,9-Epoxide of the Mycotoxin Aflatoxin-B1 - the Ultimate Carcinogenic Species. *J. Am. Chem. Soc.* **1988**, *110*, 7929−7931.
(62) Yun, B. H.; Rosenquist, T. A.; Nikolic, J.; Dragicevic, D.; Tomic, K.; Jelakovic, B.; Dickman, K. G.; Grollman, A. P.; Turesky, R. J. Human formalin-fixed paraffin-embedded tissues: an untapped specimen for

https://doi.org/10.1021/acsomega.3c01328
ACS Omega 2023, 8, 14841−14854

biomonitoring of carcinogen DNA adducts by mass spectrometry. *Anal. Chem.* **2013**, *85*, 4251−4258.

https://doi.org/10.1021/acsomega.3c01328
ACS Omega 2023, 8, 14841−14854